Theoretical and Experimental Analysis of Ionization Equilibria in Ovomucoid Third Domain†

William R. Forsyth,‡ Michael K. Gilson,§ Jan Antosiewicz,|| Olav R. Jaren,‡ and Andrew D. Robertson*,‡

Department of Biochemistry, The University of Iowa, Iowa City, Iowa 52242, Center for Advanced Research in Biotechnology, National Institute of Standards and Technology, 9600 Gudelsky Drive, Rockville, Maryland 20850, and Department of Biophysics, The University of Warsaw, 02-089, Warsaw, Poland

Received January 26, 1998; Revised Manuscript Received April 16, 1998

ABSTRACT: 2D-NMR experiments were used to determine the pK_a values ranging from 8.0 to ≥11.1 of seven basic residues in turkey ovomucoid third domain (OMTKY3) and were compared to values predicted as described by Antosiewicz et al. [(1996) *Biochemistry 35*, 7819−7833]. Lys 13, 29, and 34 were previously attributed with increasing the acidity of numerous acidic residues [Schaller, W., and Robertson, A. D. (1995) *Biochemistry 34*, 4714−4723]. These interactions were expected to raise the pK_a values of those basic groups; however, the pK_a values of Lys 13 and 34 are less than the model compound values. The pK_a values of the other basic residues are greater than the model compound values and, unlike the acidic residues, all are surprisingly insensitive to salt. While the calculations properly predict the direction of most of the pK_a shifts and provide valuable insight into the possible molecular origins of the interactions that perturb pK_a values, there is a tendency to overestimate the magnitude of the shifts and their salt dependence. Interestingly, the shapes of both the calculated and observed transitions are often more complex than expected for a simple titration, suggesting that pK_a values at many sites are changing during the transition. Differences between predicted and experimental pK_a values and titration profiles for some residues may be due to as yet uncharacterized structural changes at the extremes of pH.

Protein function and stability are intimately linked to the protonation equilibria of ionizable groups. For example, residues with significantly altered pK_a values, relative to model compounds, are often found at or near ligand-binding sites and the active sites of enzymes, with the shifts being essential for catalytic activity (*1*−*6*). These pK_a shifts are driven by interactions with charged groups and dipoles, hydrogen bonding, and solvent environment. Hence, pK_a perturbations serve as a sensitive probe of local environments within a protein. Moreover, NMR-based measurements of ionization equilibria in proteins present a rare opportunity to monitor quantitatively the energetics of a protein at multiple sites simultaneously. These equilibria are thus a rich source of information regarding the relationship between protein structure and function.

With the goal of understanding the role of ionizing residues in modulating protein stability and reactivity, the accurate prediction of ionization equilibria is currently of considerable interest. To this end, several approaches have been developed to predict ionization equilibria in proteins. Many models utilize solutions of the linearized Poisson−Boltzmann (PB) equation. In this approach, the protein is treated as a low dielectric body surrounded by solvent ions in a high dielectric medium. A free energy is calculated that reflects the change in electrostatic energy of ionizing a group in the protein environment relative to solution. This electrostatic free energy includes the contribution of permanent dipoles, any other pH-independent electric field in the protein such as from bound ions, and the presence of other titrating groups. These approaches attempt to accurately predict pK_a values and provide insight into the molecular origins of the pK_a perturbations.

In principle, a significant strength of these computational models is the opportunity to compare the predicted and experimental values. These comparisons serve one of two purposes: (1) they examine the validity of the physical model and (2) facilitate interpretation of the experimental values. Moreover, NMR can be used to derive information about multiple equilibria simultaneously, thus providing the basis for a more rigorous comparison than cases where a single pK_a is the subject of study. In practice, few proteins are stable to the extremes of pH necessary for determination of many experimental pK_a values.

The present study combines theoretical modeling and experimental determination of the ionization equilibria in turkey ovomucoid third domain (OMTKY3).[1] By virtue of its stability over a wide range of solution conditions (*7*−*10*)

†This work was supported by the National Institute of Standards and Technology and the National Institutes of Health (GM 46869 to A.D.R. and GM 54053 to M.K.G.).

* To whom correspondence should be addressed. Phone: 319-335-6515. Fax: 319-335-9570. E-mail: andy-robertson@uiowa.edu.

‡ The University of Iowa.

§ National Institute of Standards and Technology.

|| The University of Warsaw.

[1] Abbreviations: δ_A, chemical shift of the fully unprotonated species; δ_{HA}, chemical shift of the fully protonated species; δ_{obs}, observed chemical shift; ^{1}H NMR, proton nuclear magnetic resonance spectroscopy; pK_a, pH at which half of a population is ionized; *n*, Hill coefficient; OMTKY3, turkey ovomucoid third domain; rmsd, root-mean-square deviation; TOCSY, total correlation spectroscopy; TSP, sodium 3-(trimethylsilyl) propionate-2,2,3,3-d_4.

S0006-2960(98)00187-1 CCC: $15.00
Published on Web 05/28/1998

and the availability of X-ray and NMR-derived structures (*11*−*13*), OMTKY3 serves as an excellent system for the study of electrostatic interactions. The ionization equilibria of nearly all ionizable groups can be experimentally determined and compared to theoretical values.

The pK_a values of all six carboxyl groups in OMTKY3 have been determined (*14*). The pK_a values of Asp 7, Glu 19, and Asp 27 are significantly perturbed from the model compound values. These perturbations were originally attributed to stabilizing hydrogen bonds (*14*), although recent electrostatic calculations emphasize the role of long-range interactions (*15*). Many of the long-range interactions are with basic groups whose pK_a values are expected to be perturbed by the same interactions. The current study extends the experimental and computational examination of ionization equilibria in OMTKY3 into the neutral and alkaline pH range.

MATERIALS AND METHODS

Materials. Turkey ovomucoid third domain was purified as described by Swint and Robertson (*8*) from domestic turkey eggs (*Maleagris gallopavo*), a gift from Theis Farms (New Haven, IA). Deuterium oxide (99.9 atom %) and sodium 3-(trimethylsilyl) propionate-2,2,3,3-d_4 (98 atom %) were from Cambridge Isotope Laboratories (Cambridge, MA). Standardized pH buffers of 4, 7, 10, and 11 were from VWR Scientific (West Chester, PA) and Fisher Scientific (Pittsburgh, PA). Reagent grade potassium chloride was from EM Science (Gibbstown, NJ). Certified calcium hydroxide was from Fisher Scientific (Pittsburgh, PA).

Sample Preparation. A stock solution of approximately 2 mM OMTKY3 was prepared by dissolving lyophilized protein in 90% H_2O/10% D_2O (v/v) containing the concentration of potassium chloride and 0.5 mM TSP as an internal chemical shift standard. The pH of the stock solution was adjusted using concentrated HCl and KOH. The pH was measured at room temperature using an Orion Research pH meter (model 611) with a 3 mm Ingold combination electrode (Wilmad Glass Company; Buena, NJ) standardized at two points. A degassed saturated solution of $CaOH_2$ at 25 °C served as a pH 12.42 standard (*16*). Sample pH was measured both before and after the experiment. Reported pH values are not corrected for the deuterium isotope effect. The reversibility of the titrations was assessed by acidifying the stock solution after titration to alkaline pH.

NMR Spectroscopy. All TOCSY (*17*) spectra were acquired using a Nalorac Cryogenics Corporation (Martinex, CA) IDT500 5 mm triple resonance probe on a Varian UNITY spectrometer, located in the University of Iowa College of Medicine NMR facility, operating at a ^1H frequency of 499.726 MHz. The carrier frequency was set on the water signal. Solvent suppression was achieved by continuous-wave irradiation of the solvent resonance during the 2.2 s relaxation delay. The spectral width and mixing time was 6000 Hz and 80 ms, respectively. Each experiment consisted of four transients with 2048 time-domain points and either 165 or 330 increments in the indirectly detected dimension. All experiments were performed at 25 °C as determined by a methanol standard (*18*).

NMR data were processed using Varian software installed on a Sun Microsystems SparcStation 2 workstation. The time-domain data was weighted using an unshifted Gaussian filter prior to the Fourier transformation. The Gaussian time constants were 0.079 and 0.025 s in the directly and indirectly detected dimensions, respectively. The final digital resolution was 2.93 Hz/point in both dimensions and estimated uncertainties in chemical shifts are 0.007 ppm in ω_2 and 0.013 ppm in ω_1.

Determination of Apparent pK_a Values. The pH dependences of the proton chemical shift data were fit by nonlinear least-squares analysis (*19*, *20*) to a modified Hill equation (*21*, *14*) to determine an apparent ionization constant, pK_a:

$$\delta_{obs} = \delta_A[1 + 10^{n(pK_a - pH)}]^{-1} + \delta_{HA}[1 - (1 + 10^{n(pK_a - pH)})^{-1}] \quad (1)$$

where δ_{obs} is the observed chemical shift at a given pH; δ_A and δ_{HA} are the chemical shifts of the fully unprotonated and protonated species, respectively; and n is the Hill coefficient, a measure of cooperativity.

Accessible Surface Area. The solvent accessible surface area of OMTKY3 was determined using the Lee and Richards solvent-accessibility algorithm (*22*) as implemented by ACCESS (Scott R. Presnell, Zymogenetics, Seattle, WA) using a probe radius of 1.4 Å and a slice width of 0.25 Å.

Computational Methods. The computational methods have been described and validated relative to experiment in previous publications (*15*, *23*). The methods are summarized here. The charge states of the ionizable groups are computed with an algorithm (*24*) that is based upon statistical thermodynamic theory, essentially a binding polynomial, that is described elsewhere (*24*−*26*). This theory requires as input the interaction energies among the ionizable groups of the protein, and the difference between the energy of ionizing each group in the otherwise neutral protein, relative to the energy of ionizing it in bulk solvent. These energies are all assumed to be electrostatic in nature, and are computed by the Poisson−Boltzmann (PB) model (*27*−*33*). A series of PB calculations, two for each ionizable group, yields a matrix of interactions that is used with the binding polynomial to compute the ionization states as a function of pH. The energy calculations rely upon the structure of the protein as determined by X-ray crystallography or NMR, as well as a number of other parameters.

The full set of partial atomic charges appropriate to the neutral state of each group is taken as the starting point in modeling ionization. Ionization is then represented as the addition or subtraction of a unit charge to one atom of the group. The atomic charges used here (*23*) are based upon the CHARMm, version 22.0, polar-hydrogen-only parameters (Molecular Simulations Inc. Waltham, MA, CHARMm, version 22, 1992), and the radii are based upon the OPLS nonbonded parameter set (*34*).

Hydrogen coordinates are calculated for X-ray and NMR structures by the same procedure (*15*). First, tautomeric forms are assigned to neutral histidines and rotational orientations are assigned to carboxylic acids. The arbitrary default here is to assume the proton is on ND1 of the neutral form of histidine. For carboxylic acids, the default is to place the proton on the oxygen that occurs second in the file of atomic coordinates. For the C-termini of peptides, the proton is linked to the OXT atom in the neutral form. The HBUILD (*35*) command of CHARMM, version 23.1 (*36*), is used to

Table 1: NMR Proton Chemical Shifts, Measured pK_as, and Hill Coefficients of Basic Groups in OMTKY3 at 25 °C[a]

		~0.015 M KCl[b]				0.5 M KCl			
residue	proton	δ_A (ppm)	$\Delta\delta$ (ppm)	pK_a	*n*	δ_A (ppm)	$\Delta\delta$ (ppm)	pK_a	*n*
LeuN 1	$C_\alpha H$	3.45	0.58	7.96 (0.04)	0.88 (0.02)	3.46	0.60	7.96 (0.04)	1.01 (0.11)
Tyr 11	$C_\epsilon H$	6.58	0.31	10.16 (0.05)	0.73 (0.07)	6.58	0.31	10.13 (0.07)	0.77 (0.10)
Lys 13	$C_\epsilon H$	2.00	0.61	9.86 (0.03)	0.69 (0.04)	2.03	0.48	9.87 (0.04)	0.85 (0.07)
Tyr 20	$C_\epsilon H$	6.54	0.29	11.07 (0.11)	0.57 (0.06)	6.56	0.27	11.10 (0.20)	0.73 (0.12)
Lys 29	$C_\epsilon H$	2.36	0.48	11.12 (0.02)	0.87 (0.03)	2.40	0.42	10.91 (0.04)	1.10 (0.08)
Lys 34	$C_\epsilon H$	2.69	0.34	10.13 (0.05)	0.66 (0.05)	2.70	0.39	10.12 (0.12)	0.65 (0.11)
Lys 55	$C_\epsilon H$	2.62	0.48	11.10 (0.06)	0.64 (0.04)	2.72	0.39	10.79 (0.08)	0.92 (0.08)

[a] δ_{HA}, δ_A, pK_a, and Hill coefficients, *n*, were obtained from nonlinear least-squares fits to eq 1. $\Delta\delta = \delta_{HA} - \delta_A$. Numbers in parentheses represent fitting errors at one standard deviation. The fitted pK_a values of Tyr 20, Lys 34, and Lys 55 represent lower limits for the true pK_a value and, based on model compound data, are probably within 0.2 pH units of the true pK_a. [b] Salt added in the form of the titrants over the course of the experiment.

establish energetically reasonable hydrogen positions. Finally, the energy of the system is minimized with respect to the positions of the hydrogens only by 500 steps of steepest descents energy-minimization with CHARMM.

In the electrostatic calculations, the dielectric constant of the aqueous solvent is set to 78, and that of the protein to 20 (*23*). Calculations are repeated with several different ionic strengths. The thickness of the Stern layer is 2 Å, and the temperature is set to 300 K.

Calculations were done for both a crystal structure and an ensemble of NMR structures. The crystal structure was drawn from the Protein Data Bank (*37*) entry 1PPF (*12*), which is the structure of OMTKY3 complexed with the protease leukocyte elastase. The calculations omitted the protease and included only the atoms of OMTKY3. The 50 NMR structures were drawn from the Protein Data Bank entry 1OMU (*38*). Separate electrostatic calculations were done for each structure, and the charge of each group as a function of pH was computed for each separate structure. These charges were then averaged over the ensemble of 50 structures to obtain the mean charge of each group as a function of pH. The pK_a value of each group was defined based upon these averaged charges.

The influence of each ionizable group upon the pK_a value of the other groups was obtained by artificially deleting the group in question from the matrix of interactions mentioned above. Then the binding polynomial theory is used to recompute the pK_a values of the remaining groups. These pK_a values reflect the artificial deletion of the test group from the protein, under the assumption that the mutation does not change the structure of the protein or the other energy terms. Each row in Table 4 thus gives the expected shifts in the pK_a values when the group identified on the left is deleted. Each diagonal term in Table 4 is the pK_a shift when all other groups are assumed neutral and includes the effect of desolvation and interactions with neutral polar groups. Therefore, the influence of hydrogen bonds appears in the diagonal entries while the influence of charge−charge interactions appears in the off-diagonal entries.

EXPERIMENTAL RESULTS

OMTKY3 contains 16 ionizable groups (Figure 1), nine of which titrated over the pH range covered in this study, 5.0−12.7. Of these, the pK_a of the single histidine, His 52, has been determined previously (*40*). Of the remaining ionizing groups, there are three side chain phenolic protons, a δ-guanido group, and the rest are side-chain and backbone amino protons. The δ-guanido group of Arg 21 does not appear to begin titrating until the higher pH range examined in this study.

The previously assigned ^{1}H NMR spectrum of OMTKY3 (*41*) served as a starting point for analysis of the TOCSY

Table 2: Experimental and Predicted pK_a Values and Hill Coefficients of Ionizing Groups in OMTKY3 at 25 °C, Low Salt Conditions[a]

	pK_a			*n*		
residue	expt	pred (NMR)[b]	pred (Xtal)[c]	expt	pred (NMR)[d]	pred (Xtal)[e]
LeuN 1	8.0	7.5 (0.2)	7.1	0.88	0.98	0.94
Asp 7	<2.7	3.3 (0.3)	2.9	0.72	0.56	0.71
Glu 10	4.2	3.5 (0.5)	3.4	0.92	0.62	0.70
Tyr 11	10.2	10.0 (1.0)	9.8	0.73	1.00	0.79
Lys 13	9.9	11.2 (0.3)	12.3	0.69	1.08	0.65
Glu 19	3.2	2.8 (0.3)	3.2	1.08	0.90	0.84
Tyr 20	11.1	9.9 (0.4)	9.8	0.57	0.93	0.78
Arg 21		12.8 (0.2)	12.8		0.58	0.84
Asp 27	<2.3	3.4 (0.3)	4.0	0.85	0.93	0.80
Lys 29	11.1	12.1 (0.5)	11.5	0.87	0.88	0.83
Tyr 31	>12.5	11.2 (0.9)	12.9		0.76	0.83
Lys 34	10.1	11.7 (0.9)	11.7	0.66	0.36	0.71
Glu 43	4.8	4.4 (0.2)	4.3	0.95	0.88	0.83
His 52	7.5	6.2 (0.2)	6.3	0.93	1.01	0.93
Lys 55	11.1	11.3 (0.4)	11.1	0.64	0.83	0.76
CysC 56[f]	<2.5	2.7 (0.2)	2.7	0.87	0.86	0.92

[a] Experimental values (expt) of basic groups were obtained at approximately 15 mM KCl. Values of acidic groups, determined at 10 mM KCl, are from Schaller and Robertson (*14*). Values for Tyr 31 and His 52 were determined at 0.2 M KCl (*40*). Predicted values (pred) are based on 20 mM salt. Fitted pK_a values of Tyr 20, Lys 34, and Lys 55 represent lower limits for the true pK_a value and, based on model compound data, are probably within 0.2 pH units of the true pK_a. [b] Predicted pK_a values based on NMR structures (1OMU). Numbers in parentheses indicate rmsd of pK_a values for the 50 structures. [c] Predicted pK_a values based on crystal structure 1PPF. [d] Sum of influence of all ionizable groups on Hill coefficients based on NMR structures, 20 mM salt. [e] Hill coefficients computed at transition midpoints using crystal structure 1PPF. [f] pK_a of carboxyl group. Residue forms disulfide bridge with Cys 24.

Table 3: Linear Regression Analysis of Predictive Models

	rmsd	slope	*y*-intercept
null model	1.3	0.74	1.8
new null model[a]	0.73	0.90	0.51
computations (NMR)[b]	0.89	0.97	0.19
computations (Xtal)[c]	1.1	1.0	0.13

[a] New null model values taken from Antosiewicz et al. (*15*). [b] Computations based NMR structures 1OMU at 20 mM salt. [c] Computations based on crystal structure 1PPF at 20 mM salt.

Table 4: Analysis of the Origins of the pK_a Shifts at 20 mM Salt[a]

	LeuN1	Asp 7	Glu 10	Tyr 11	Lys 13	Glu 19	Tyr 20	Arg 21	Asp 27	Lys 29	Tyr 31	Lys 34	Glu 43	His 52	Lys 55	CysC 56
LeuN 1	0.04	**0.11**	0.07	0.00	−0.05	0.06	0.00	**−0.11**	0.05	−0.03	0.00	−0.09	0.03	−0.01	−0.05	0.06
Asp 7	**−0.15**	**−0.61**	**0.33**	0.00	−0.08	0.08	0.00	**−0.16**	0.03	−0.03	0.00	**−0.41**	0.01	−0.05	−0.03	0.03
Glu 10	−0.04	**0.46**	**−0.71**	0.00	**−0.67**	**0.12**	0.00	**−0.10**	0.02	−0.03	0.00	**−0.56**	0.01	−0.02	−0.02	0.02
Tyr 11	0.00	**0.42**	**0.79**	**−0.80**	**−0.96**	**0.23**	0.05	**−0.20**	0.05	−0.08	0.01	**−2.02**	**0.13**	0.00	−0.03	0.04
Lys 13	0.00	**0.17**	**0.47**	**0.37**	**1.19**	**0.19**	0.03	**−0.10**	0.01	−0.01	0.02	−0.01	0.06	0.00	−0.01	0.01
Glu 19	−0.06	0.03	0.03	0.00	**−0.20**	**−1.19**	0.00	**−0.53**	0.01	−0.03	0.00	**−0.38**	0.00	−0.04	−0.09	0.03
Tyr 20	0.00	0.03	0.02	0.03	−0.02	**0.12**	**−0.28**	**−0.15**	0.07	**−0.14**	0.01	−0.03	0.06	0.00	**−0.61**	**0.24**
Arg 21	0.00	**0.11**	0.07	**0.11**	−0.01	**0.53**	**0.15**	**1.23**	0.04	−0.01	0.04	−0.09	0.02	0.00	−0.01	0.09
Asp 27	−0.05	0.02	0.01	0.00	−0.02	0.02	0.00	−0.04	**−0.85**	**−0.66**	0.00	−0.04	0.03	**−0.17**	−0.06	**0.14**
Lys 29	0.00	0.03	0.02	0.02	0.00	0.02	**0.13**	−0.02	**0.65**	**1.85**	**0.63**	−0.01	**0.26**	0.00	−0.01	**0.15**
Tyr 31	0.00	0.07	0.04	0.05	−0.02	0.04	**0.12**	−0.05	**0.62**	**−0.66**	**0.77**	−0.01	**0.54**	0.00	−0.04	**0.12**
Lys 34	0.00	**0.58**	**0.41**	**1.58**	**−0.12**	**0.55**	0.06	**−0.49**	0.03	−0.01	0.03	**2.29**	0.02	0.00	−0.02	0.04
Glu 43	−0.02	0.05	0.06	0.00	−0.06	0.04	0.00	−0.03	**0.18**	**−0.28**	0.00	−0.05	**−0.22**	−0.04	−0.04	0.05
His 52	**−0.10**	0.06	0.04	0.00	−0.04	0.06	0.00	**−0.12**	**0.23**	**−0.13**	0.00	−0.08	0.06	**0.63**	**−0.24**	**0.89**
Lys 55	0.00	0.02	0.01	0.01	−0.01	0.07	**0.60**	**−0.13**	0.05	−0.05	0.03	−0.02	0.02	0.00	**1.02**	**0.40**
CysC 56	−0.06	0.01	0.00	0.00	−0.02	0.03	0.00	−0.08	0.04	**−0.13**	0.00	−0.03	0.00	**−0.99**	**−0.39**	**−1.52**

[a] For nondiagonal entries, each row gives the expected shifts in the pK_a values of the groups listed in the column heading, based on the NMR structures (1OMU), when the group identified on the left is deleted. For example, the deletion of LeuN 1 is expected to increase the pK_a of Asp 7 by 0.11 pK_a units. Diagonal terms are the expected shifts when all other groups are neutral. For example, with all other groups neutral, the pK_a of Asp 7 is expected to be 0.61 pK_a units less than the model compound value. Values are in units of pK_a shift with large shifts (≥0.10 pK_a units in magnitude) in bold.

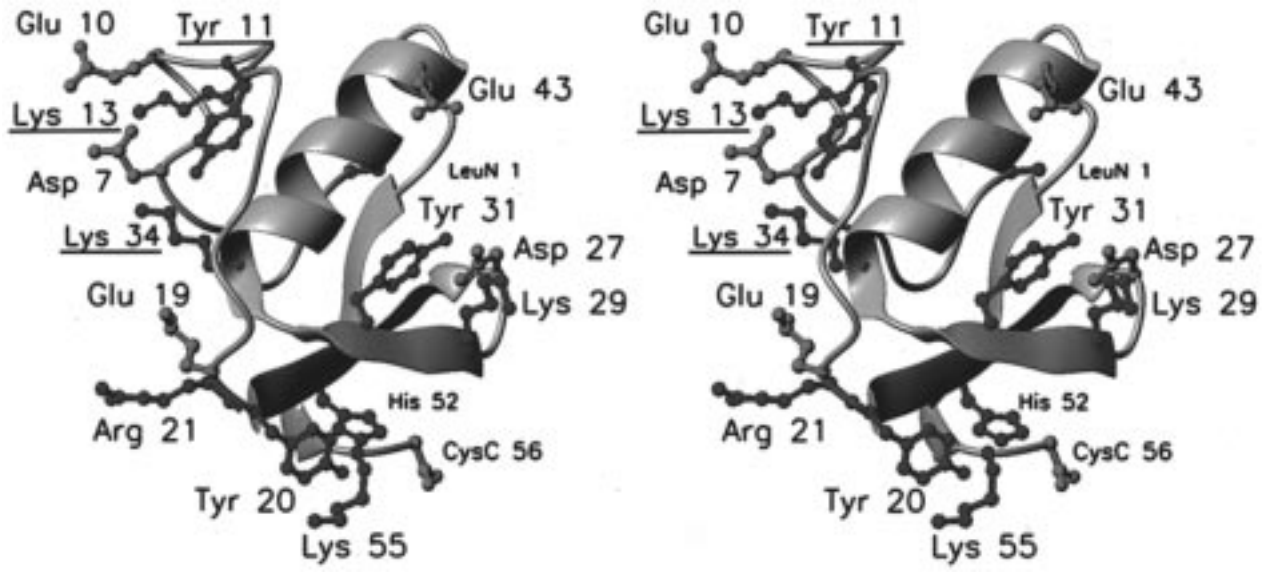

FIGURE 1: Stereo ribbon diagram of third domain. Ionizing groups are shown in ball-and-stick form. Red residues have pK_a values of <6 (*14*), while blue residues, covered in this study, have pK_a values of >6. Underlined residues are discussed in more detail later. The figure was prepared using MOLMOL (*39*).

titration data. All upfield changes in chemical shifts with increasing pH, 0.3−0.6 ppm (Figure 2), are similar to the changes observed in small peptides (*42*) and other proteins (*43*−*45*). All of the observed transitions were completely reversible.

Incomplete transitions were observed for Tyr 20, Lys 34, and Lys 55 due to peak overlap (Figures 3 and 4). As a result, the fitted pK_a values for these residues (Table 1) represent lower limits for the true pK_a value but are probably within 0.2 pH units of the true pK_a since the transitions appear to be greater than 80% complete, based on model compound data. Given the fitted pK_a values, the experiments would have to be continued at least to pH 14 in order to establish the high pH baselines for the lysine and tyrosine residues.

Low Salt Studies. To examine the largest possible pK_a perturbations in native OMTKY3, experiments were executed in the presence of minimal added salt. Thus, the concentrations of added salt ranged from 0.5 mM at pH 7.5 to approximately 15 mM at pH 12.4, reflecting salt added as TSP and in the form of the titrants.

Amino Terminus. The $C_\alpha H$ proton resonance of Leu 1 is very sensitive to the titration of the amino group, and cross-peaks involving the $C_\alpha H$ proton resonance of Leu 1 are readily resolved over the entire pH range covered in this study. A full transition was observed with the resolved resonances shifting upfield approximately 0.6 ppm upon titration of the amino group (Figure 3). The fitted pK_a of 8.0 (Table 1) is close to the model compound value of 7.5 (*46*).

(a) Tyrosine Residues. The $C_\epsilon H$ proton chemical shifts were used to monitor the titration of the hydroxyl group. Titration profiles of only two (Tyr 11 and 20) of the three tyrosine residues could be determined since no $C_\epsilon H$ cross-peaks could be discerned for Tyr 31. However, the pK_a for this residue has been previously reported as being higher

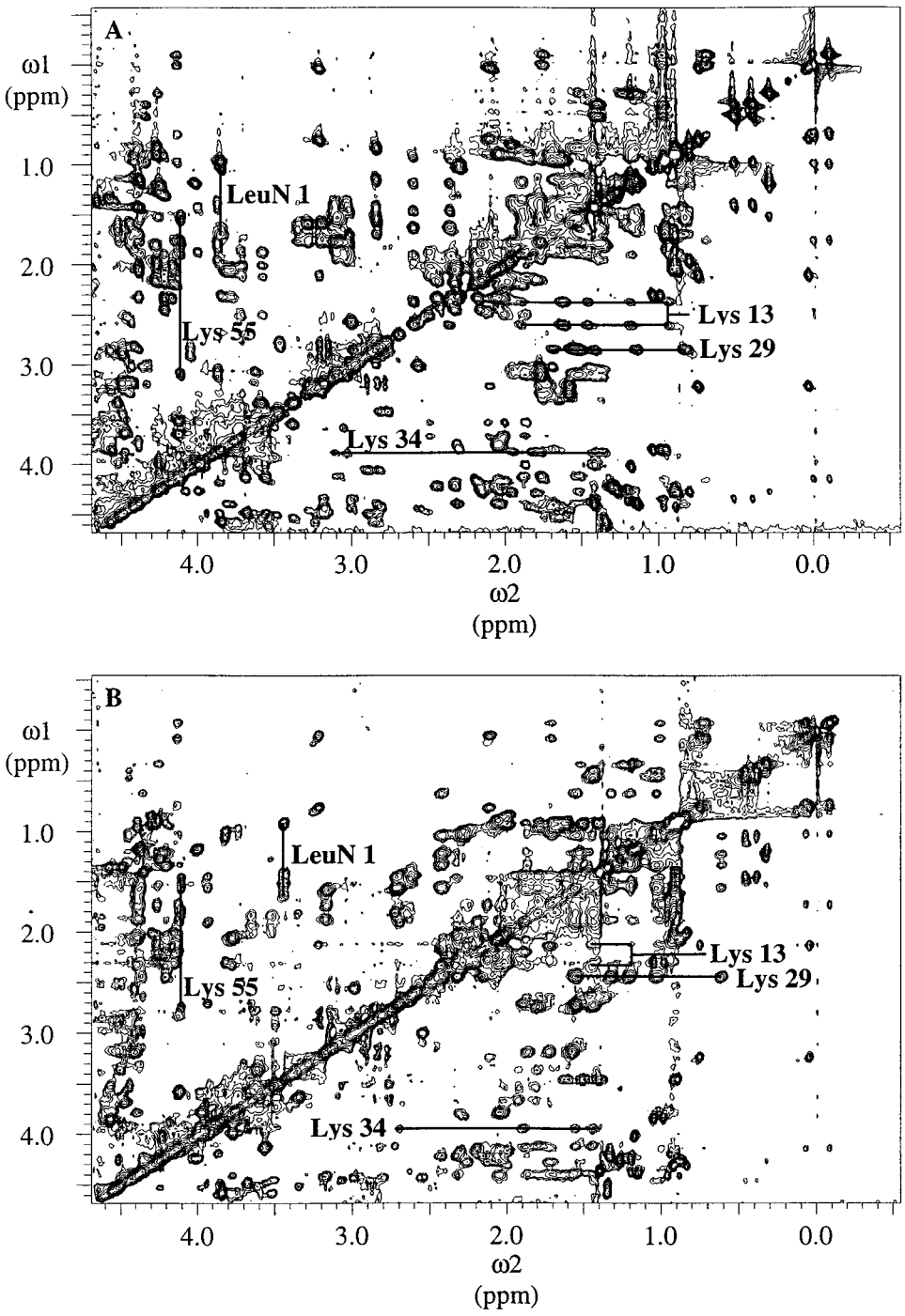

FIGURE 2: Expansion of the aliphatic regions of TOCSY spectra (τ_{mix} of 80 ms) of 2 mM OMTKY3 at 25 °C at pH 7.50 (A) and pH 12.14 (B) in ~15 mM salt. Spin systems are indicated by lines. For LeuN 1, Lys 34, and Lys 55, the lines are along the $C_\alpha H$ chemical shift while for Lys 13 and Lys 29 the lines are along the $C_\epsilon H$ chemical shifts.

than 12.5 (*40*). Tyr 11 and 20 exhibited upfield changes in chemical shifts of about 0.3 ppm (Figure 3). Neither titration profile is complete. The fitted pK_a values of both Tyr 11 and 20 and 10.2 and 11.1, respectively (Table 1), are higher than the model compound value of 9.6 (*46*).

(b) Lysine Residues. The $C_\epsilon H$ protons are sensitive to the titration to the ϵ-amino group (*43*, *47*, *48*). Hence, the pH dependence of the $C_\epsilon H$ resonances of Lys 13, 29, 34, and 55 was monitored. All residues exhibited resolved TOCSY cross-peaks involving the $C_\epsilon H$ protons and, at least, the $C_\gamma H$ and $C_\delta H$ protons. The fitted pK_a values for Lys 29 and 55 are both approximately 11.1, significantly elevated with respect to the model compound value of 10.4 (*46*). On the other hand, Lys 13 and 34 have depressed pK_a values of 9.9 and 10.1, respectively.

High Salt Studies. One mean of ascertaining the significance of electrostatic interactions occurring through the solvent is to utilize the masking effects of salt. In contrast to the behavior of the carboxyl groups (*14*), the pK_a values of the basic groups, with the exception of Lys 29 and 55, are surprisingly insensitive to 0.5 M salt (Table 1). Hence, any contributing electrostatic interactions appear to occur through the protein even though many of the residues are well-exposed to solvent.

Hill Coefficients. The pH dependencies of the chemical shifts were fit to a modified Hill equation (eq 1). The Hill

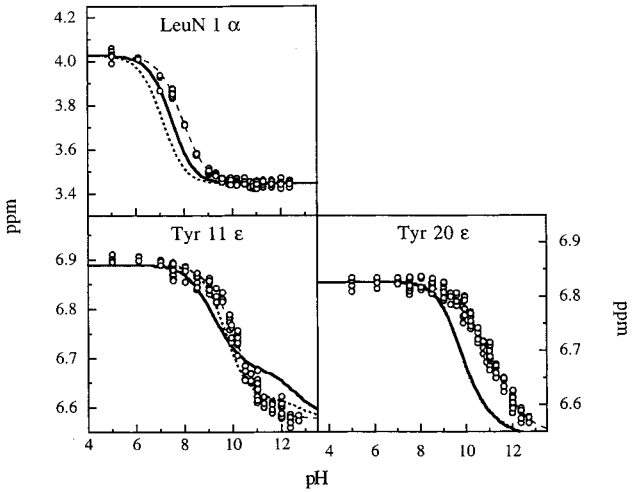

FIGURE 3: pH dependences of OMTKY3 chemicals shifts (○) at 25 °C ($I \approx 15$ mM) for the amino terminus and two tyrosine residues. α and ε designate the monitored proton resonance. Data points represent chemical shift measurements from all resolvable cross-peaks as well as from multiple independent measurements. Dashed lines represent least-squares fits to eq 1. Bold and smaller dashed lines are predicted titration profiles based on the NMR and crystal structures, respectively. The predicted titration profiles overlap in the case of Tyr 20.

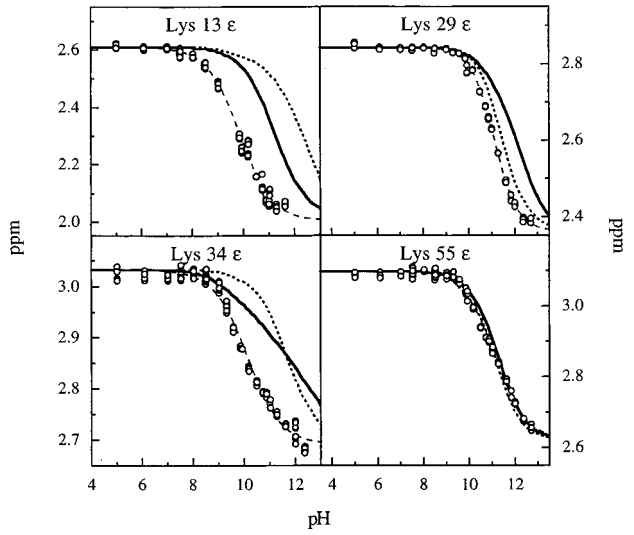

FIGURE 4: pH dependences of OMTKY3 chemicals shifts (○) at 25 °C ($I \approx 15$ mM) for the lysine residues with ε designating the monitored resonance. Data points represent chemical shift measurements from all resolvable cross-peaks as well as from multiple independent experiments. Dashed lines represent least-squares fits to eq 1. Bold and smaller dashed lines are predicted titration profiles based on the NMR and crystal structures, respectively.

coefficient, *n*, reflects interactions with other groups ionizing over the same pH range. An alternative treatment of coupled equilibria takes into account all of the microscopic equilibrium constants involved in the observed macroscopic equilibrium (*49*). This treatment, however, requires identification of all ionizable groups contributing to the observed equilibrium. Such knowledge is lacking at present for OMTKY3. Consequently, the Hill coefficient serves as a phenomenological description of cooperativity for those curves that deviate from simple titration behavior.

The Hill coefficient for the amino terminus was 0.9 and 1.0 at low- and high-salt conditions, respectively, and overlapped at one confidence interval. The values of *n* for side-chain groups at low ionic strength were 0.6−0.9 while at high ionic strength the range of *n* values increased to 0.7−1.1 (Table 1). An elevation of *n* reflects the screening of electrostatic interactions by salt. Surprisingly, the values of *n* for Lys 34 and Tyr 11 are insensitive to salt.

In most cases, omission of *n* from the fitting equation yielded pK_a values that were statistically identical to the previous values even though the variance of the fit becomes larger (not shown). In the case of Tyr 20 and Lys 55, the fitted pK_a values show a modest decrease to 10.8 ± 0.1 and 10.9 ± 0.1, respectively, when *n* is omitted from the fit.

Calculated Values. The electrostatic calculations yield values for the fraction protonated at a given ionizable group with respect to pH. These estimates have been cast as chemical shifts in Figures 3 and 4 using the fitted chemical shifts for the fully protonated and deprotonated species, δ_A and δ_{HA}, respectively, in eq 1. Table 2 compares experimentally determined pK_a values for the ionizable groups in OMTKY3 with the values derived from calculations based on both the NMR and crystal structures (PDB files 1OMU and 1PPF, respectively). Values based on the NMR structures represent the average of 50 structures, thereby allowing for the calculation of an rmsd for every group. The NMR and crystal based pK_a values overlap with a few exceptions (including Lys 13, Asp 27, and Tyr 31).

While the calculations tend to overestimate the magnitude of the pK_a shifts, particularly for Lys 13 and Lys 34, there is good agreement in terms of the direction of the perturbations. There are two notable exceptions. In the case of Lys 13, the calculations predict a significantly increased pK_a, relative to the model compound value, while the experimental results indicate a decreased pK_a. In the other case, the calculations predict that the pK_a of Glu 43 might be slightly depressed when, in fact, the pK_a is perceptibly increased.

The tendency of the calculations to overestimate the magnitude of the pK_a shifts depends on the experimental ionic strength. Figure 5A indicates that the calculated values shift on the order of 0.3 pK_a units between ionic strengths of 0 and 50 mM. The values become generally insensitive to ionic strengths above 50 mM. The differences between the predicted and experimental values at both low and high ionic strengths are not explained by the predicted ionic strength dependence.

Included in Table 2 are the Hill coefficients calculated at the midpoints of the transitions according to the values based on the NMR and crystal structures. Figure 5B illustrates the calculated ionic strength dependence of the Hill coefficients. The Hill coefficients of several residues do not approach unity with increasing ionic strength; this indicates that strong electrostatic interactions occur through the protein interior. Of particular interest is the Hill coefficient of Tyr 11, which denotes intensifying interactions with increasing ionic strength.

DISCUSSION

Experimental Considerations. One concern in the present study is the possibility of protein unfolding at high pH. However, the presence of substantial upfield-shifted methylene resonances at high pH coupled with the systematic progression of δ_{obs} strongly suggests that OMTKY3 is folded throughout the study. Persistence of the second set of

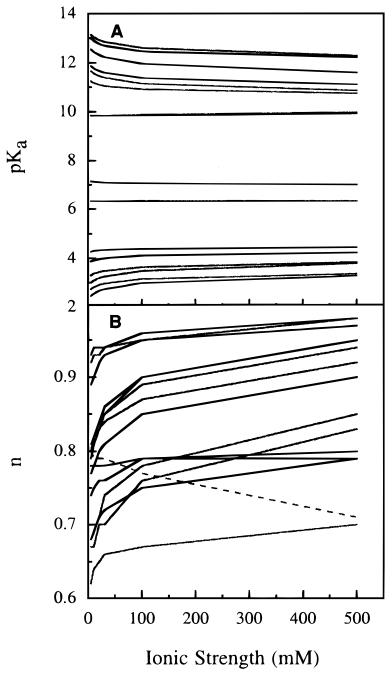

FIGURE 5: Ionic strength dependence of computed pK_a values (A) and Hill coefficients (B) based on the crystal structure 1PPF. Dashed line in panel B represents Tyr 11.

resonances for Lys 13 at pH 12 (Figure 2B) due to the ring current effects of Tyr 11 further indicates that OMTKY3 was properly folded. The integrity of the folded protein at alkaline pH is further substantiated by preliminary circular dichroism and differential scanning calorimetry experiments (unpublished results).

An assumption in the data analysis is that the ionization of a site can be accurately monitored by the chemical shift of the protons separated from that site by two or three covalent bonds. This is well documented for peptides and proteins (*43*−*45*). However, the reporter proton in a protein may be sensitive not only to its ionizing substituent group (intrinsic effects) but also to the ionization of other nearby groups (extrinsic effects). The combination of intrinsic and extrinsic effects will alter the shape of the transition region, thereby influencing the fitted values for pK_a and *n*. Examination of the chemical shifts for nonionizing residues in OMTKY3 that are near an ionizable group suggests that extrinsic effects, if present, contribute on the order of a few hundredths of a part per million.

Some of the experiments were conducted in the presence of minimal added salt in an effort to observe the maximum possible pK_a perturbations. The reported ionic strength in these experiments does not take into account the possibility of residual salt ions present in the purified protein preparation. Consequently, the weak salt dependence of the basic pK_a values may in fact reflect higher salt concentrations than expected. Moreover, the high protein concentrations employed in the studies may also contribute to the screening of electrostatic interactions (*44*). However, the present studies were performed under conditions similar to those of Schaller and Robertson (*14*) where significant pK_a perturbations and strong salt dependencies were observed for the acidic groups.

Lysines and Tyrosines in Other Proteins. The lysine pK_a values in OMTKY3 range from 9.9 to greater than 11.1. This is well within the range observed with other proteins. For example, nearly full transitions were observed for the lysine residues in basic pancreatic trypsin inhibitor with the fitted pK_a values being 10.6 for the three NMR-equivalent residues (Lys 15, 21, and 46) and 10.8 for Lys 41 (*43*). In the case of the apo-form of Calbindin D_{9k}, the 10 lysine residues exhibited fitted pK_a values ranging from 10.5 to 12.1 (*44*). The recent study of the B1 and B2 immunoglobin G-binding domains of protein G reported fitted pK_a values from 10.7 to greater than 11 with most lysines falling into the latter category (*45*). In a staphylococcal nuclease mutant, the pK_a of a lysine fully buried in the hydrophobic core was calculated to be less than 6.4 (*50*). While this value is not typical of the pK_a shift observed in wild-type proteins, it does illustrate the extent to which a pK_a might become perturbed due to environmental factors.

Many of the tyrosine pK_a values reported in the literature were determined spectrophotometrically and are therefore macroscopic values that cannot be attributed to individual tyrosine residues. NMR has been applied to the study of tyrosine residues in relatively few instances. In *Streptomyces* subtilisin inhibitor, all three tyrosine residues were found to have elevated pK_a values of 11.0, 11.8, and $\geq$12.6 with full transitions observed for the two lower values (*51*). The pK_a of $\geq$12.6 was attributed to a tyrosine acting as a proton donor in a hydrogen bond. Four tyrosines in the catalytic subunit of aspartate transcarbamoylase were found to have pK_a values of 9.8, 10.2, 10.3, and 10.9 with the titration behavior being completely reversible (*52*). A tyrosine in basic pancreatic trypsin inhibitor was found to have a pK_a of 9.8 (*43*). Values of approximately 11, >11, and >12 were determined for the three tyrosines in the B1 and B2 immunoglobulin G-binding domains of protein G (*45*). A study that incorporated Hill analysis reported that the pK_a values of seven tyrosine residues in staphylococcal nuclease ranged from 9 to 11 (*53*). Another study of staphylococcal nuclease determined the pK_a of Tyr 85, which plays a role in exonucleolytic catalysis, to be 9.5 (*54*). A study of the titration behavior of tyrosine residues in myoglobins found that the titration of one tyrosine was consistent with two pK_a values of 9.8 and 11.6, another tyrosine had a pK_a of 10.6, and a third residue did not begin to titrate even at pH 12 (*55*).

Most of the lysine and tyrosine pK_a values in the previous studies are lower limits of the true pK_a since full transitions were rarely observed. Additionally, most studies did not use Hill analysis to analyze the breadth of the transitions, and therefore may have missed important information regarding the cooperativity of ionization. With the exception of the Calbindin D_{9k} and aspartate transcarbamoylase studies, the reversibility of the transitions was not examined. Nevertheless, the range of values observed for OMTKY3 is consistent with these studies.

Model Comparison. Ionization equilibria provide one of the few experimental measures of the accuracy of electrostatic calculations, which are widely used to study a variety of phenomena including ligand binding and interactions between membranes and proteins. However, no systematic comparative studies of methods to predict pK_a values have been done and studies combining critical analysis of experimental and predicted ionization equilibria are rare (*44*, *45*, *56*, *57*). Separate laboratories try different improvements

in the calculations with the result that some predicted pK_a values are improved and others are made worse. However, the general trend over the years is that the root-mean-square deviation between predicted and experimental pK_a values has decreased.

The overall agreement between experimental and calculated values in such studies varies. For acidic groups, agreement between experimental and predicted values is better for aspartate than glutamate residues (*15*, *45*). Many methods tend to overestimate the pK_a of basic groups, especially lysine residues (*44*, *56*, *57*). These differences in agreement may result from any of several factors, both computational and experimental.

One exemplary study examined several factors that can significantly influence the accuracy of the predicted values (*56*). This study systematically investigated the effects of varying atomic radii, atomic coordinates, and charge parameters and found that these can have significant effects on the predicted ionization equilibria. Other studies have mentioned the dependency of the predicted values on the structural models used in the calculations (*15*, *23*, *26*, *58*). A structural issue yet to be resolved is accounting for possible conformational changes that might accompany the titration of ionizing groups in proteins (*58*, *59*). Conformational changes have been found in a number of proteins (see discussion in refs *60* and *61*) with changes in pH. The inclusion of limited conformational flexibility as a function of pH can increase the accuracy of predicted values (*58*, *62*).

Two approximations based on the average pK_a values found in model compounds and proteins, the "null" and "new null" models, respectively, can serve as benchmarks to evaluate computational models (*15*, *46*). Briefly, the "null" model assumes that protein structure and charged groups have no effect on the pK_a values of ionizable groups, while the "new null" model predicts that the pK_a of a given group will be the mean of the experimentally observed pK_a values for that group in a set of proteins. Analysis of scatter plots comparing predicted and experimental pK_a values is one method to assess the global accuracy of a model. Table 3 reports the statistical analysis of scatter plots for the present calculations based on the NMR and crystal structures of OMTKY3 as well as the null and new null models.

The calculations are considerably more accurate than the null model (rmsd of 1.3), but not quite as accurate as the new null model (rmsd of 0.73). As with some other studies, the calculations based on the NMR structures are in better agreement with experimental values (rmsd of 0.89) than the crystal structure based values (rmsd of 1.1) (*15*, *45*). However, the crystal structure has OMTKY3 complexed with human leukocyte elastase. Subtle differences in the bound structure may account for the lower agreement relative to calculations based on the NMR structures.

Origins of pK_a Perturbations. While the current predictions may not be more accurate than those of the new null model, they do provide specific information on the possible molecular origins of the pK_a perturbations. Table 4 summarizes the pK_a shifts, based on the NMR structures at 20 mM salt, among the ionizable groups in OMTKY3. These calculations suggest that long-range (>5 Å) electrostatic interactions play a more important role than one might expect by simple inspection of the structure.

(a) Amino Terminus. The pK_a of the amino terminus is not significantly shifted from the model compound value, which is consistent with its location in an unstructured region of the protein. According to the calculations, no one group is predominantly responsible for the slightly elevated pK_a; rather it results from the cumulative effects of partially compensating weak interactions.

(b) Lysine Residues. Interestingly, Lys 13 exhibited two sets of cross-peaks (Figure 2). The origin of this duplication is attributed to ring current effects of Tyr 11 (*63*), whose side chain is approximately 5 Å away (Figure 1). The high-field $C_\epsilon H$ resonance at low pH is tentatively assigned to the *pro-R* proton based on the crystal structure and the expected ring current shift due to Tyr 11. This resonance moved only approximately 0.05 ppm over the course of the titration and was not used in the pK_a determination. As Figure 1 illustrates, Lys 13 is also close to Lys 34. These three residues (Lys 13, Lys 34, and Tyr 11) form an interesting case in terms of electrostatics and will be discussed later in more detail.

Lys 29 shows a high degree of side-chain positional variability in both the crystal structure, according to the temperature factors, and the NMR structures; this would allow it to come into proximity with several groups. According to the calculations, the pK_a would be elevated 1.85 units due to some combination of desolvation and interactions with neutral polar groups (Table 4). Strong interactions of the ϵ amino group with the nearby γ carboxylate group of Asp 27 and the phenol oxygen of Tyr 31 could further elevate the pK_a of Lys 29. The calculations also suggest that Glu 43 plays a significant role in influencing the pK_a of Lys 29, even though the interaction spans approximately 8.8 Å in the crystal structure and is generally around 14 Å in the NMR structures.

According to the calculations, Tyr 20 will ionize prior to the deprotonation of Lys 55, hence stabilizing the charge of the amino group, which is a about 3.7 Å away. Experimentally though, Tyr 20 and Lys 55 have similar pK_a values and therefore deprotonate over the same pH range. The interaction among the partial charges of these two groups results in a broadened profile (Figures 3 and 4). This interaction may be reflected in the similar n values of 0.64 $\pm$ 0.04 and 0.57 $\pm$ 0.06 for Lys 55 and Tyr 20, respectively (Table 1). The combination of desolvation and interactions with neutral polar groups significantly influences the pK_a of Lys 55. The calculations also indicate that His 52 and the carboxy terminus of Cys 56 contribute to the perturbed pK_a of Lys 55, although to a lesser degree.

It is curious that the calculations tend to reproduce the pK_a values of the carboxyl groups better than the lysines. As reviewed in Table 4, the calculations suggest that the increased acidity of Asp 7, Glu 10, Glu 19, and Asp 27 results largely from stabilizing interactions with Lys 13, Lys 29, and Lys 34 over distances of 5−10 Å (*15*). One might therefore expect that the same interactions would elevate the pK_a values of these lysines, and this is precisely what the present calculations predict. However, the measurements show that these predictions are incorrect: the lysine pK_a values are near their ideal values. In addition, the lysine pK_a values are virtually independent of ionic strength, suggesting that they are influenced little by the carboxylates. In contrast, the carboxylate pK_a values rise with ionic

strength, as predicted by the electrostatic model (*15*). In summary, there appears to be an asymmetry in the interactions of the carboxylates with the lysines.

A striking similar asymmetry is found in small aminocarboxylic acids. Thus, a study of 2-, 3-, and 4-piperidinemonocarboxylic acids found that the pK_a of the amino group does not change with its distance from the carboxyl; but, in contrast, the pK_a of the carboxyl falls as it approaches the amino group, as expected from an electrostatic model (*64*). An even more counterintuitive result is found for aminocarboxylic acids in the form $NH_3^+(CH)_nCOO^-$. As n decreases, the amino group becomes less basic despite its approach to the negatively charged carboxylic, but the carboxyl becomes more acidic as predicted from an electrostatic model (*65*). These results are interesting in themselves and will be considered in more detail elsewhere. Whether they bear on the determination of pK_a shifts in proteins remains to be determined.

(c) Tyrosine Residues. As previously mentioned, Tyr 11 interacts with both Lys 13 and 34 and will be discussed in a later section.

Desolvation is attributed with increasing the pK_a of Tyr 20. With a solvent accessible surface area of only 7.9 Å^2, ionization of the hydroxyl group will be unfavorable. This counteracts the influence of Lys 55 on Tyr 20 and elevates the pK_a into the regime of Lys 55. The very high pK_a of Tyr 31 may be attributed to a short hydrogen bond between the hydroxyl hydrogen and the γ carboxyl oxygen of Asp 27, approximately 2.5 Å away according to the crystal structure. The low solvent accessible surface area of 8.4 Å^2 may also contribute. On the other hand, the calculations suggest that the pK_a elevation is due to a strong electrostatic interaction with Lys 29 and the combined influence of desolvation and interactions with neutral polar groups which contribute shifts of 0.63 and 0.77 pK_a units (Table 4).

Lys 13, Lys 34, and Tyr 11. Lys 13, 34, and Tyr 11 together form a unique cooperative triad (Figure 1) that exemplifies the potential complexity of interpreting pK_a perturbations by simple visual inspection. One might expect the pK_a of Tyr 11 to be lowered because of favorable interaction of the anion with the positive charges of the lysine side chains. This would also elevate the lysine pK_a values. However, the pK_a of Lys 13 is depressed while those of Tyr 11 and Lys 34 are elevated.

Within this triad, there are two unfavorably interacting positive charges. This unfavorable interaction will persist even if Tyr 11 were deprotonated. Of the two lysine residues, the interaction of Lys 34 with the γ carboxylate oxygen of Asp 7, approximately 5.3 Å away, would inhibit its deprotonation. Additionally, even if all other groups in the protein were neutral, the pK_a of Lys 34 would be elevated by 2.29 pK_a units. The difficulty in deprotonating Lys 34 favors a depressed pK_a for Lys 13. If the overall interaction energies among one neutral and two positive charges are less favorable than the interactions energies among one positive and two neutral charges, then it might explain Lys 13 deprotonating before Tyr 11.

This is only one possible explanation for the observed pK_a shifts and it clearly would be difficult to anticipate these shifts through structural inspection alone. Due to the cooperativity in this triad, a small error in the predicted pK_a for one of the residues would easily propagate to the other two residues.

Predicted Titration Profiles. Aside from predicting a pK_a or even a Hill coefficient, a special feature of these computations is the ability to predict titration profiles (Figures 3 and 4). Predicting the continuous change in pK_a values with respect to pH, manifested in the breadth and shape of the profile, provides considerable information about possible changes in interactions occurring during the ionization process.

As Figures 3 and 4 illustrate, agreement between the experimental and predicted profiles varies. For instance, agreement between the predicted and experimentally observed titration profiles is excellent for Lys 55 but poor in the case of Lys 34 and Tyr 11. The calculations accurately predict the shape of most profiles, but the curves are systematically shifted from those determined experimentally. This suggests that, for these residues, the calculations account for most of the electrostatic interactions but usually overestimate their magnitudes. One interesting finding from the calculations is that Hill coefficients may not capture the true complexity of a titration profile. A clear example is Tyr 11 in which the predicted *n* value of 1.00 (Table 2) belies the biphasic nature of the predicted titration profile (Figure 3).

The differences in the titration profiles based on the NMR and crystal structures, hence pK_a and *n* values, result from differences in side-chain positions. While these structural variations may be subtle, they have a significant impact on the shapes of the profiles. These profiles highlight the necessity of using accurate structures in the calculations and suggest that structural alterations (e.g., occurring during the titration) could have profound effects.

ACKNOWLEDGMENT

The authors thank Drs. Robert Cohen, Kenneth P. Murphy, and Earle Stellwagen for careful reading of the manuscript. Certain commercial equipment or materials are identified in this paper in order to specify the methods adequately. Such identification does not imply recommendation or endorsement by the National Institute of Standards and Technology, nor does it imply that the materials or equipment identified are necessarily the best available for the purpose.

REFERENCES

1. Perutz, M. F. (1978) *Science 201*, 1187−1191.
2. Nakanishi, K., Balogh-Nair, V., Arnaboldi, M., Tsujimoto, K., and Honig, B. (1980) *J. Am. Chem. Soc. 102*, 7945−7947.
3. Hol, W. G. J. (1985) *Prog. Biophys. Mol. Biol. 45*, 149−195.
4. Kakitani, H., Kakitani, T., Rodman, H., and Honig, B. (1985) *Photochem. Photobiol. 41*, 471−479.
5. Matthew, J. B. (1985) *Annu. Rev. Biophys. Biophys. Chem. 14*, 387−417.
6. Honig, B. H., Hubbell, W. L., and Flewelling, R. F. (1986) *Annu. Rev. Biophys. Biophys. Chem. 15*, 163−193.
7. Ardelt, W., and Laskowski, M., Jr. (1991) *J. Mol. Biol. 220*, 1041−1053.
8. Swint, L., and Robertson, A. D. (1993) *Protein Sci. 2*, 2037−2049.
9. Swint-Kruse, L. and Robertson, A. D. (1995) *Biochemistry 34*, 4724−4732.
10. Arrington, C. B., and Robertson, A. D. (1997) *Biochemistry 36*, 8686−8691.
11. Read, R. J., Fujinaga, M., Sielecki, A. R., and James, M. N. G. (1983) *Biochemistry 22*, 4420−4433.

12. Bode, W., Wei, A.-Z., Huber, R., Meyer, E., Travis, J., and Neumann, S. (1986) *EMBO J. 5*, 2453−2458.
13. Krezel, A. M., Darba, P., Robertson, A. D., Fejzo, J., Macura, S., and Markley, J. L. (1994) *J. Mol. Biol. 242*, 203−214.
14. Schaller, W., and Robertson, A. D. (1995) *Biochemistry 34*, 4714−4723.
15. Antosiewicz, J., McCammon, J. A., and Gilson, M. K. (1996) *Biochemistry 35*, 7819−7833.
16. Bates, R. (1973) *Determination of pH: Theory and Practice*, 2nd Ed., 59−104, John Wiley and Sons, New York.
17. Bax, A. (1989) *Methods Enzymol. 176*, 151−168.
18. Van Geet, A. L. (1968) *Anal. Chem. 40*, 2227−2229.
19. Johnson, M. L., and Frasier, S. G. (1985) *Methods Enzymol. 117*, 301−342.
20. Johnson, M. L., and Faunt, L. M. (1992) *Methods Enzymol. 210*, 1−37.
21. Markley, J. L. (1975) *Acc. Chem. Res. 8*, 70−80.
22. Lee, B., and Richards, F. M. (1971) *J. Mol. Biol. 55*, 379−400.
23. Antosiewicz, J., McCammon, J. A., and Gilson, M. K. (1994) *J. Mol. Biol. 238*, 415−436.
24. Gilson, M. K. (1993) *Proteins*: *Struct., Funct., Genet. 15*, 266−282.
25. Schellman, J. A. (1975) *Biopolymers 14*, 999−1018.
26. Bashford, D., and Karplus, M. (1990) *Biochemistry 29*, 10219−10225.
27. Warwicker, J., and Watson, H. C. (1982) *J. Mol. Biol. 157*, 671−679.
28. Gilson, M. K., Rashin, A., Fine, R., and Honig, B. (1985) *J. Mol. Biol. 184*, 503−516.
29. Klapper, I., Hagstrom, R., Fine, R., Sharp, K., and Honig, B. (1986) *Proteins*: *Struct., Funct., Genet. 1*, 47−59.
30. Gilson, M. K., Sharp, K. A., and Honig, B. H. (1988) *J. Comput. Chem. 9*, 327−335.
31. Gilson, M. K., and Honig, B. (1988) *Proteins*: *Struct., Funct., Genet. 4*, 7−18.
32. Honig, B., Sharp, K., and A.-S Yang (1993) *J. Phys. Chem 97*, 1101−1109.
33. Madura, J. D., Davis, M. E., Gilson, M. K., Wade, R. C., Luty, B. A., and McCammon, J. A. (1994) in *Reviews in Computational Chemistry* (Lipkowitz, K. B., and Boyd, D. B., Eds.), Vol. 5, pp 229−267, VCH Publishers, New York.
34. Jorgensen, W. L., and Tirado-Rives, J. (1988) *J. Am. Chem. Soc. 110*, 1657−1666.
35. Brünger, A. T., and Karplus, M. (1988) *Proteins*: *Struct., Funct., Genet. 4*, 148−156.
36. Brooks, B. R., Bruccoleri, R. E., Olafson, B. D., States, D. J., Swaminathan, S., and Karplus, M. (1983) *J. Comput. Chem. 4*, 187−217.
37. Bernstein, F. C., Koetzle, T. F., Williams, G. J. B., Meyer, E. F. B., Jr., Brice, M. D., Rodgers, J. R., Kennard, O., Shimanouchi, T., and Tasumi, M. (1977) *J. Mol. Biol. 112*, 535−542.
38. Hoogstraten, C. G., Choe, S., Westler, W. M., and Markley, J. L. (1995) *Protein Sci. 4*, 2289−2299.
39. Koradi, R., Billeter, M., and Wüthrich, K. (1996) *J. Mol. Graphics 14*, 51−55.
40. Ortiz-Polo, G. (1985) M. S. Thesis, Purdue University.
41. Robertson, A. D., Westler, W. M., and Markley, J. L. (1988) *Biochemistry 27*, 2519−2529.
42. Bundi, A., and Wüthrich, K. (1977) *FEBS Lett. 77*, 11−14.
43. Brown, L. R., De Marco, A., Wagner, G., and Wüthrich, K. (1976) *Eur. J. Biochem. 62*, 103−107.
44. Kesvatera, T., Jönsson, B., Thulin, E., and Linse, S. (1996) *J. Mol. Biol. 259*, 828−839.
45. Khare, D., Alexander, P., Antosiewicz, J., Bryan, P., Gilson, M., and Orban, J. (1997) *Biochemistry 36*, 3580−3589.
46. Nozaki, Y., and Tanford, C. (1967) *Meth. Enzymol. 11*, 715−734.
47. Bradbury, J. H., and Brown L. R. (1973) *Eur. J. Biochem. 40*, 565−576.
48. Brown, L. R., and Bradbury, J. H. (1975) *Eur. J. Biochem. 54*, 219−227.
49. Shrager, R. I., Cohen, J. S., Heller, S. R., Sachs, D. H., and Schechter, A. N. (1972) *Biochemistry 11*, 541−547.
50. Stites, W. E., Gittis, A. G., Lattman, E. E., and Shortle, D. (1991) *J. Mol. Biol. 221*, 7−14.
51. Fujii, S., Akasaka, K., and Hatano, H. (1981) *Biochemistry 20*, 518−523.
52. Cohen, R. E., Takama, M. and Schachman, H. K. (1992) *Proc. Natl. Acad. Sci. U.S.A. 89*, 11881−11885.
53. Chinami, M., and Shingu, M. (1989) *Arch. Biochem. Biophys. 270*, 126−136.
54. Grissom, C. B., and Markley, J. L. (1989) *Biochemistry 28*, 2116−2124.
55. Wilbur, D. J., and Allerhand, A. (1976) *J. Biol. Chem. 251*, 5187−5194.
56. Bashford, D., Case, D. A., Dalvit, C., Tennant, L., and Wright, P. E. (1993) *Biochemistry 32*, 8045−8056.
57. Tishmack, P. A., Bashford, D., Harms, E., and Van Etten, R. L. (1997) *Biochemistry 36*, 11984−11994.
58. You, T. J., and Bashford, D. (1995) *Biophys. J. 69*, 1721−1733.
59. Baptista, A. M., Martel, P. J., and Petersen, S. B. (1997) *Proteins 27*, 523−544.
60. Yang, F., and Phillips, G. N., Jr. (1996) *J. Mol. Biol. 256*, 762−774.
61. Robinson, V. L. (1997) Ph.D. Thesis, The University of Iowa.
62. Alexov, E. G., and Gunner, M. R. (1997) *Biophys. J. 74*, 2075−2093.
63. Johnson, C. E., and Bovey, F. A. (1958) *J. Chem. Phys. 29*, 1012−1014.
64. Hansen, L. D., and Lewis, E. A. (1973) *J. Phys. Chem. 77*, 286−289.
65. Edward, J. T., Farrell, P. G., Job, J. L., and Poh, B.-L. (1978) *Can. J. Chem. 56*, 1122−1129.

BI980187V